Triaza-based amphiphilic chelators: synthetic route, *in vitro* characterization and *in vivo* studies of their Ga(III) and Al(III) chelates

Arsénio de Sá[1], M. Isabel M. Prata[2], Carlos F. G. C. Geraldes[3], João P. André[1*]

[1] Centro de Química, Campus de Gualtar, Universidade do Minho, 4710-057 Braga, Portugal

[2] IBILI, Faculdade de Medicina, Universidade de Coimbra, Coimbra, Portugal

[3] Departamento de Ciências da Vida, Faculdade de Ciências e Tecnologia, e Centro de Neurociências e Biologia Celular, Universidade de Coimbra, 3001-401 Coimbra, Portugal

* Tel: +351 253 604 385; Fax: +351 253 604 382; Email: jandre@quimica.uminho.pt

Keywords: triaza, orthogonal protection, amphiphilic, gallium, aluminum, radiopharmacy

Abstract

Radiogalium chelates are important for diagnostic imaging in nuclear medicine (PET and γ-scintigraphy). Micelles are adequate colloidal vehicles for the delivery of therapeutic and diagnostic agents to organs and tissues. In this paper we describe the synthesis and *in vitro* and *in vivo* studies of a series of micelles-forming Ga(III) chelates targeted for the liver. The amphiphilic ligands are based on NOTA (NOTA = 1,4,7-triazacyclonoane-*N,N'N''*-triacetic acid) and bear a α-alkyl chain in one of the pendant acetate arms (the size of the chain changes from four to fourteen carbon atoms). A multinuclear NMR study (^{1}H, ^{13}C, ^{27}Al and ^{71}Ga) gave some insights into the structure and dynamics of the metal chelates in solution, consistent with their rigidity and octahedral or pseudo-octahedral geometry. The critical micellar concentration of the chelates was determined using a fluorescence method and ^{27}Al NMR spectroscopy (Al(III) was used as a surrogate of Ga(III)), both showing similar results and suggesting that the chelates of NOTAC6 form pre-micellar aggregates. The logP (octanol-water) determination showed enhancement of the lipophilic character of the Ga(III) chelates with the increase of the number of carbons in the α-alkyl chain. Biodistribution and γ-scintigraphic studies of the ^{67}Ga(III) labeled chelates were performed on Wistar rats, showing higher liver uptake for [^{67}Ga](NOTAC8) in comparison to [^{67}Ga](NOTAC6), consistent with a longer α-alkyl chain and a higher lipophilicity. After 24 hours both chelates were completely cleared off from the tissues and organs with no deposition in the bones and liver/spleen. [^{67}Ga](NOTAC8) showed high kinetic stability in blood serum.

1. Introduction

Radiogallium chelates are of great interest in the field of medical imaging. ^{67}Ga ($t_{1/2}$ = 3.25 days), a γ emitter, is useful for γ-scintigraphy, while ^{68}Ga ($t_{1/2}$ = 68 min), a β^+ emitter, is adequate for positron emission tomography (PET). $^{67/68}$Ga(III), with a very well known coordination chemistry, allows easy radiopharmaceutical preparation, as the radiometal can be very rapidly inserted in adequate molecules, contrarily to the covalently bound PET radioisotopes ^{18}F or ^{11}C, leading to a minimum loss of activity [1].

Ga(III) is a hard Lewis acid that forms thermodynamically stable chelates with ligands that are hard Lewis bases, often with a coordination number of six. The main requirements for a Ga(III)-based radiopharmaceutical agent are the thermodynamic stability towards hydrolysis and the kinetic inertness during the period of clinical use in order to avoid ligand exchange with the blood serum proteins, such as transferrin (Tf). Ga(III) is quite similar to the high spin Fe(III) ion in what concerns their ionic radii (62 pm and 65 pm, respectively, when hexacoordinated), charge and coordination chemistry. Transferrin has two binding sites for Fe(III), that have also high affinity for Ga(III) (log $K_{(Ga\text{-}Tf)}$ = 20.3 [2]), and is present in high concentrations in plasma, 2.5 x 10^{-3} M. Thus, when ^{67}Ga(III) is injected in the form of gallium citrate (or another low stability complex) more than 90% of this metal is complexed by transferrin.

Several chelators for Ga(III) have been proposed, the majority of them being hexadentate [1, 3-11]. Among the chelators, triaza macrocycles display high conformational and size selectivity towards Ga(III) ions. The high thermodynamic stability of the Ga(III) chelates of nine-membered triaza ligands is due to the adequate fit of the relatively small cation in the macrocyclic cavity. The high thermodynamic stabilities of Ga(III) chelates of NOTA-like ligands are illustrated respectively by log

$K_{Ga(NOTA)}$ = 30.98 and log $K_{Ga(NODASA)}$ = 30.9(0.2) (NOTA = 1,4,7-triazacyclonoane-*N*,*N'N''*-triacetic acid; NODASA = 1,4,7-triazacyclonoane-*N*-succinic acid-*N'N''*-diacetic acid) [9, 12]. Their high resistance against exchange of Ga(III) in blood serum and acid-catalyzed dissociation has been demonstrated [9].

Some of the ligands currently used for the preparation of radiopharmaceuticals of Ga(III) are bifunctional, meaning that they present a functionality that allows covalent coupling to a targeting vector (e.g. peptides), besides binding the metal ion. The coupling to the targeting moiety requires that the pro-chelator, often bearing carboxylic acid groups, has the possibility of orthogonal protection [13].

Micelles are colloidal aggregates that have been extensively used as drug carriers to improve pharmacokinetic properties or the bioavailability of the drug, to increase the target-to-background ratio of the drug or to deliver hydrophobic drugs [14-17]. These self-assembly constructs accumulate in macrophage-rich tissues, such as liver and spleen, undergoing endocytosis/phagocytosis [14, 18]. Micelles loaded with suitable reporter groups can have application in medical imaging. Gd(III)-containing micelles are of interest as MRI contrast agents due to the possibility of delivery of high payloads of paramagnetic ion to the biological receptors and to the expected increase in their relaxivity as a consequence of the slowing down of the rotational dynamics of the chelates upon aggregation [19, 20]. By their turn, radio-labeled (^{125}I, ^{111}In, ^{153}Sm) micelles have been employed in γ-scintigraphic studies for the visualization of macrophage-rich tissues such as lymph nodes, liver and spleen [21-24].

In this work we envisaged the synthesis and the study of micelles-forming triaza chelates of Ga(III) potentially interesting for diagnosis in nuclear medicine. The synthetic route of this series of NOTA-based chelators, with one of the acetate pendant arms bearing a α-alkyl substituent with a variable number of carbon atoms (from four to

fourteen - NOTAC6, NOTAC8, NOTAC10, NOTAC16, see Scheme 1) makes use of an orthogonal protection strategy, allowing their coupling to targeting biomolecules.

A multinuclear NMR study (^{1}H, ^{13}C, ^{27}Al and ^{71}Ga) gave an insight on the structure and dynamic behavior of the metal chelates in solution. Al(III) chelates were used as models of the analogous Ga(III) chelates, due to the more suitable magnetic resonance properties of aluminum (100% abundance and fairly good receptivity) [4]. The variation of the half-width of the ^{27}Al NMR signal with concentration allowed the assessment of the critical micellar concentration (cmc) of the amphiphilic Al(III) chelates, consistent with the quadrupolar nature of the Al(III) ion. The cmc results were confirmed using a fluorescent method based on the use of ANS (8-anilino-1-napthalene sulfonic acid) [25].

A very important indicator for *in vivo* applications is the measurement of the rate of exchange of Ga(III) in blood serum under physiological conditions [26]. For this purpose, the stability of the ^{67}Ga(III) labeled chelates in blood serum was investigated. Biodistribution and γ-scintigraphic studies of the ^{67}Ga(III) labeled chelates were performed in Wistar rats.

2. Experimental

2.1. Materials and methods

Analytical grade reagents were purchased from Sigma-Aldrich, Fluka, Acros Organics, Macrocyclics and Chematech. [^{67}Ga](citrate) was purchased from CIS-BIO (Gif-sur- Yvette, France). The reactions were monitored by thin layer chromatography (TLC) on aluminum plates coated with silica gel 60 F_{254} (Macherey-Nagel).

Chromatography separations were performed on silica gel Whatman 230-240 Mesh. The NMR spectra were recorded on a Varian Unity Plus 300 spectrometer or on

a Bruker Avance III 400 spectrometer. The ^{1}H NMR spectra were assigned using the two-dimensional COSY technique. The ^{1}H chemical shifts are reported in ppm, relative to tetramethylsilane (TMS) or sodium 2,2-dimethylsilapentane-5-sulfonate (DSS) and the following abbreviations are used: s = singlet; s_b = broad singlet; d = doublet; dd = double doublet; t = triplet; t_b = broad triplet; m = multiplet; m_b = broad multiplet. ^{27}Al NMR spectra were recorded at 104.261 MHz (on the Bruker Avance III 400 spectrometer) using the signal of $[Al(H_2O)_6]^{3+}$ at 0 ppm as reference. ^{71}Ga NMR spectra were recorded at 122.026 MHz (on the same spectrometer) using the signal of $[Ga(H_2O)_6]^{3+}$ at 0 ppm as reference. pH measurements were performed on a pH meter Crison micro TT 2050 with an electrode Mettler Toledo InLab 422. Mass spectra (ESI^{+}) were performed on a VG Autospec M spectrometer or on a Finnigan LXQ MS Detector.

2.2. Synthetic procedures

2.2.1. Diphenyldiazomethane (1)

In a 1 L flask, benzophenonehydrazone (10.0 g, 51.0 mmol), yellow mercuric oxide (26.9 g, 124 mmol), anhydrous sodium sulfate (11.5 g, 81.0 mmol) and a saturated ethanol solution of KOH (3.80 mL) were suspended in ethyl ether (154 mL) and stirred for 75 min, according to the method published by Miller [27]. The solution was filtered and the solvent was evaporated under vacuum at room temperature. The dark red oil obtained was dissolved in petroleum ether 40-60ºC and filtered once again. The solvent was evaporated at room temperature and the residue was frozen. When heated to room temperature, the diphenyldiazomethane (DDM, **1**) afforded dark red crystals (9.86 g, 50.8 mmol) in a yield of 99.6%.

2.2.2. 2-bromohexanoate *tert*-butyl ester (2a)

A solution of *tert*-butyltrichloroacetimidate (TBTA) (5.00 g, 22.9 mmol) in 11.0 mL of cyclohexane was added dropwise during 10 min to a solution of 2-

bromohexanoic acid (0.815 mL, 5.72 mmol) in 10.0 mL of dichloromethane (DCM). During the addition, a white precipitate was formed, which was dissolved with the addition of 1.25 mL of *N,N*-dimethylacetamide. A catalyst, boron trifluoride ethyl etherate ($BF_3.OEt_2$) (0.700 mL), was added to the reaction and a new white precipitate was formed. The reaction was stirred during three days, according to the method published by Nicolle *et al.* [20]. The precipitate was removed by filtration and the solution was concentrated. The oil obtained was purified by chromatography (cyclohexane/ethyl acetate 7:3) originating a volatile brown oil **2a** (1.16 g 4.62 mmol) in a yield of 80.5%. ^{1}H NMR (300 MHz, $CDCl_3$, TMS, δ(ppm)): 0.91 (3H, t, J = 7.5 Hz, $(CH_2)_2C\underline{H}_3$), 1.29-1.40 (4H, m, $(C\underline{H}_2)_2CH_3$), 1.48 (9H, s, $C(C\underline{H}_3)_3$), 1.86-2.10 (2H, m, $C\underline{H}_2$ AB$\underline{X}$), 4.10 (1H, t, J = 7.5 Hz, C$\underline{H}$ AB$\underline{X}$).

2.2.3. 2-bromohexanoate benzhydryl ester (2b)

A solution of 2-bromohexanoic acid (3.70 mL, 26.0 mmol) in 160 mL of acetone was added to a solution of compound **1** (4.50 g, 23.2 mmol) in 160 mL of acetone. The reaction was stirred during 13 h in an ice bath and 10 h at room temperature. The solution was then concentrated and the yellow oil obtained was purified by chromatography (cyclohexane/ethyl acetate 4:1) affording the expected ester **2b** with a yield of 93.1% (7.82 g, 21.6 mmol). ^{1}H NMR (300 MHz, $CDCl_3$, TMS, δ(ppm)): 0.88 (3H, t, J = 6.6 Hz, $(CH_2)_2C\underline{H}_3$), 1.22-1.48 (4H, m, $(C\underline{H}_2)_2CH_3$), 1.97-2.18 (2H, m, $C\underline{H}_2$ AB$\underline{X}$), 4.33 (1H, t, J = 7.2 Hz, C$\underline{H}$ AB$\underline{X}$), 6.92 (1H, s, $C\underline{H}(Ph)_2$), 7.32-7.40 (10H, m, $CH(\underline{Ph})_2$).

2.2.4. 2-bromooctanoate benzhydryl ester (2c)

The title compound was prepared according to the method described for the preparation of **2b**, starting from 2-bromooctanoic acid and using cyclohexane/ethyl acetate (9.5:0.5) as eluent in the chromatography. The compound **2c** (5.10 g, 13.1

mmol) was obtained with a yield of 99.8%. ^{1}H NMR (300 MHz, $CDCl_3$, TMS, δ(ppm)): 0.89 (3H, t, J = 6.6 Hz, $(CH_2)_4C\underline{H}_3$), 1.24-1.30 (8H, m, $(C\underline{H}_2)_4CH_3$), 1.96-2.18 (2H, m, $C\underline{H}_2$ AB$\underline{X}$), 4.34 (1H, t, J = 7.2 Hz, C$\underline{H}$ AB$\underline{X}$), 6.92 (1H, s, C$\underline{H}(Ph)_2$), 7.34-7.39 (10H, m, CH($\underline{Ph}$)$_2$). ^{13}C NMR (75.43 MHz, $CDCl_3$, TMS, δ(ppm)): 13.97 (1C, $(CH_2)_4\underline{C}H_3$), 22.40-31.41 (4C, $(\underline{C}H_2)_4CH_3$), 34.88 (1C, $\underline{C}H_2$ AB$\underline{X}$), 46.12 (1C, $\underline{C}$H AB$\underline{X}$), 78.18 (1C, $\underline{C}H(Ph)_2$), 127.02-139.45 (12C, CH($\underline{Ph}$)$_2$), 168.69 (1C, CH$\underline{C}$O).

2.2.5. 2-bromodecanoate benzhydryl ester (2d)

The title compound was prepared according to the method described for the preparation of **2b**, starting from 2-bromodecanoic acid and using cyclohexane/ethyl acetate (4:1) as eluent in the chromatography. The compound **2d** (6.78 g, 16.2 mmol) was obtained with a yield of 98.8%. ^{1}H NMR (300 MHz, $CDCl_3$, TMS, δ(ppm)): 0.95 (3H, t, J = 6.3 Hz, $(CH_2)_6C\underline{H}_3$), 1.20-1.42 (12H, m, $(C\underline{H}_2)_6CH_3$), 2.00-2.22 (2H, m, $C\underline{H}_2$ AB$\underline{X}$), 4.38 (1H, t, J = 7.8 Hz, C$\underline{H}$ AB$\underline{X}$), 6.97 (1H, s, C$\underline{H}(Ph)_2$), 7.33-7.45 (10H, m, CH($\underline{Ph}$)$_2$).

2.2.6. 2-bromohexadecanoate *tert*-butyl ester (2e)

The title compound was prepared according to the method described for the preparation of **2a**, starting from 2-bromohexadecanoic acid. The purification was performed by recrystallization with methanol affording the ester **2e** (3.11 g, 7.94 mmol) with a yield of 73.5%. ^{1}H NMR (300 MHz, $CDCl_3$, TMS, δ(ppm)): 0.89 (3H, t, J = 5.1 Hz, $(CH_2)_{12}C\underline{H}_3$), 1.26 (24H, s, $(C\underline{H}_2)_{12}CH_3$), 1.49 (9H, s, $C(C\underline{H}_3)_3$), 1.87-2.10 (2H, m, $C\underline{H}_2$ AB$\underline{X}$), 4.11 (1H, t, J = 9.9 Hz, C$\underline{H}$ AB$\underline{X}$).

2.2.7. 2-bromohexadecanoate benzhydryl ester (2f)

The title compound was prepared according to the method described for the preparation of **2b**, starting from 2-bromohexadecanoic acid and using cyclohexane/ethyl acetate (4:1) as eluent in the chromatography. The compound **2f** (6.04 g, 12.0 mmol)

was obtained with a yield of 93.8%. ^{1}H NMR (300 MHz, $CDCl_3$, TMS, δ(ppm)): 0.93 (3H, t, J = 6.3 Hz, $(CH_2)_{12}C\underline{H}_3$), 1.20-1.42 (24H, m, $(C\underline{H}_2)_{12}CH_3$), 1.98-2.20 (2H, m, $C\underline{H}_2$ AB$\underline{X}$), 4.35 (1H, t, J = 7.2 Hz, C$\underline{H}$ AB$\underline{X}$), 6.94 (1H, s, C$\underline{H}(Ph)_2$), 7.32-7.42 (10H, m, CH($\underline{Ph}$)$_2$). ^{13}C NMR (75.43 MHz, $CDCl_3$, TMS, δ(ppm)): 14.11 (1C, $(CH_2)_{12}\underline{C}H_3$), 22.67-31.90 (12C, $(\underline{C}H_2)_{12}CH_3$), 34.89 (1C, $\underline{C}H_2$ AB$\underline{X}$), 46.12 (1C, $\underline{C}$H AB$\underline{X}$), 78.19 (1C, $\underline{C}H(Ph)_2$), 127.03-139.46 (12C, CH($\underline{Ph}$)$_2$), 168.68 (1C, CH$\underline{C}$O).

2.2.8. 1,4,7-triazacyclononane-*N*-hexanoate *tert*-butyl ester (3a)

A solution of **2a** (0.747 g, 2.97 mmol) in 17.0 mL of DCM was added dropwise to a solution of 1,4,7-triazacyclononane (0.500 g, 3.87 mmol) in 26.0 mL of DCM. The reaction was stirred during 24 h. The white precipitate was filtered off and the solution was concentrated. The yellow residue obtained was purified by chromatography (DCM/EtOH 10:0 -> 7:3 and DCM/EtOH/NH_3 7:3:0.5) giving rise to compound **3a** (0.191 g, 0.638 mmol) with a yield of 21.5%. ^{1}H NMR (300 MHz, $CDCl_3$, TMS, δ(ppm)): 0.95 (3H, t, J = 6.6 Hz, $(CH_2)_2C\underline{H}_3$), 1.30-1.45 (4H, m, $(C\underline{H}_2)_2CH_3$), 1.47 (9H, s, $C(C\underline{H}_3)_3$), 1.70-1.85 (2H, m, $C\underline{H}_2$ AB$\underline{X}$), 2.60-3.65 (12H, m, en), 4.62 and 4.94 (1H, dd, J = 9.6 Hz and J = 10.2 Hz, C$\underline{H}$ AB$\underline{X}$). m/z (ESI^+) calculated for $C_{16}H_{34}N_3O_2$ $(M+H)^+$ 300.27. Found 300.25.

2.2.9. 1,4,7-triazacyclononane-*N*-hexanoate benzhydryl ester (3b)

The title compound was prepared according to the method described for the preparation of **3a**, starting from **2b**. The yellow residue obtained was purified by chromatography (DCM/EtOH 9:1). The compound **3b** (0.107 g, 0.261 mmol) was obtained with a yield of 32.2%. ^{1}H NMR (300 MHz, $CDCl_3$, TMS, δ(ppm)): 0.83 (3H, t, J = 6.3 Hz, $(CH_2)_2C\underline{H}_3$), 1.20-1.37 (4H, m, $(C\underline{H}_2)_2CH_3$), 1.46-1.86 (2H, m, $C\underline{H}_2$ AB$\underline{X}$), 2.69-3.42 (12H, m, en), 4.43 and 4.76 (1H, dd, J = 9.9 and 9.6 Hz, C$\underline{H}$ AB$\underline{X}$), 6.86 (1H, s, C$\underline{H}(Ph)_2$), 7.20-7.30 (10H, m, CH($\underline{Ph}$)$_2$).

2.2.10. 1,4,7-triazacyclononane-*N*-octanoate benzhydryl ester (3c)

The title compound was prepared according to the method described for the preparation of **3a**, starting from **2c** and was obtained with 35.2% yield (0.126 g, 0.288 mmol). ^{1}H NMR (300 MHz, $CDCl_3$, TMS, δ(ppm)): 0.86 (3H, t, J = 5.7 Hz, $(CH_2)_4C\underline{H}_3$), 1.21-1.40 (8H, m, $(C\underline{H}_2)_4CH_3$), 1.50-1.90 (2H, m, $C\underline{H}_2$ AB$\underline{X}$), 2.72-3.26 (12H, m, en), 4.47 and 4.77 (1H, dd, J = 9.6 and 9.9 Hz, C$\underline{H}$ AB$\underline{X}$), 6.90 (1H, s, C$\underline{H}(Ph)_2$), 7.27-7.36 (10H, m, CH($\underline{Ph}$)$_2$).

2.2.11. 1,4,7-triazacyclononane-*N*-hexadecanoate *tert*-butyl ester (3e)

The title compound was prepared according to the method described for the preparation of **3a**, starting from **2d**. Compound **3e** (0.132 mg, 0.300 mmol) was obtained with a yield of 17.2%. ^{1}H NMR (300 MHz, $CDCl_3$, TMS, δ(ppm)): 0.87 (3H, t, J = 6.9 Hz, $(CH_2)_{12}C\underline{H}_3$), 1.25 (24H, s, $(C\underline{H}_2)_{12}CH_3$), 1.45 (9H, s, $C(C\underline{H}_3)_3$), 1.68-1.81 (2H, m, $C\underline{H}_2$ AB$\underline{X}$), 2.76-3.56 (12H, m, en), 4.59 and 4.92 (1H, dd, J = 9.9 Hz, C$\underline{H}$ AB$\underline{X}$).

2.2.12. 1,4,7-triazacyclononane-*N*-hexanoate *tert*-butyl ester-*N'*-*N''*-diacetate *tert*-butyl ester (4a)

Potassium carbonate (0.279 g, 2.02 mmol) and 2-bromoacetate *tert*-butyl ester (0.142 mL, 0.964 mmol) were added to a solution of **3a** (0.144 g, 0.481 mmol) in 21.0 mL of acetonitrile (MeCN). After 24 h, the remaining potassium carbonate was filtered off and the solution was concentrated. The yellow oil obtained was purified by chromatography (DCM/EtOH 7:3). The compound **4a** (0.147 g, 0.278 mmol) was obtained with a yield of 57.8%. ^{1}H NMR (300 MHz, $CDCl_3$, TMS, δ(ppm)): 0.89 (3H, t, J = 7 Hz, $(CH_2)_2C\underline{H}_3$), 1.24-1.39 (4H, m, $(C\underline{H}_2)_2CH_3$), 1.45 (27H, s, $C(C\underline{H}_3)_3$), 1.50-1.70 (2H, m, $C\underline{H}_2$ AB$\underline{X}$), 2.58-3.40 (17H, m, en, $C\underline{H}_2CO$, C$\underline{H}$ AB$\underline{X}$). m/z (ESI$^+$) calculated for $C_{28}H_{54}N_3O_6$ $(M+H)^+$ 528.40. Found 528.42.

2.2.13. 1,4,7-triazacyclononane-*N*-hexanoate benzhydryl ester-*N'*-*N''*-diacetate *tert*-butyl ester (4b)

The title compound was prepared according to the method described for the preparation of **4a**, starting from **3b**. The compound **4b** (0.137 g, 0.215 mmol) was obtained with a yield of 82.4%. ^{1}H NMR (300 MHz, $CDCl_3$, TMS, δ(ppm)): 0.84 (3H, t, J = 6.9 Hz, $(CH_2)_2C\underline{H}_3$), 1.20-1.40 (4H, m, $(C\underline{H}_2)_2CH_3$), 1.44 (18H, s, $C(C\underline{H}_3)_3$), 1.45-1.84 (2H, m, $C\underline{H}_2$ AB<u>X</u>), 2.60-3.60 (16H, m, en and $C\underline{H}_2CO$), 4.80 (1H, C<u>H</u> AB<u>X</u>), 6.88 (1H, s, $C\underline{H}(Ph)_2$), 7.27-7.33 (10H, m, $CH(\underline{Ph})_2$). ^{13}C NMR (100.613 MHz, $CDCl_3$, TMS, δ(ppm)): 13.81 (1C, $(CH_2)_2\underline{C}H_3$), 22.49 (1C, $CH_2\underline{C}H_2CH_3$), 27.87-28.06 (6C, $C(\underline{C}H_3)_3$), 28.75 (1C, $\underline{C}H_2CH_2CH_3$), 31.15 (1C, $\underline{C}H_2$ AB<u>X</u>), 50.62-68.12 (8C, en and $\underline{C}H_2CO$), 59.21 (1C, <u>C</u>H AB<u>X</u>), 77.00 (1C, $\underline{C}H(Ph)_2$), 81.62-85.28 (2C, $\underline{C}(CH_3)_3$), 126.52-139.88 (12C, $CH(\underline{Ph})_2$), 164.03 (1C, CH<u>C</u>O), 170.93-172.06 (2C, $CH_2\underline{C}O$). m/z (ESI^+) calculated for $C_{37}H_{56}N_3O_6$ $(M+H)^+$ 638.41691. Found 638.41671.

2.2.14. 1,4,7-triazacyclononane-*N*-octanoate benzhydryl ester-*N'*-*N''*-diacetate *tert*-butyl ester (4c)

The title compound was prepared according to the method described for the preparation of **4a**, starting from **3c**. The compound **4c** (0.093 g, 0.140 mmol) was obtained with a yield of 48.6%. ^{1}H NMR (300 MHz, $CDCl_3$, TMS, δ(ppm)): 0.86 (3H, t, J = 6.3 Hz, $(CH_2)_4C\underline{H}_3$), 1.22-1.29 (8H, m, $(C\underline{H}_2)_4CH_3$), 1.45 (18H, s, $C(C\underline{H}_3)_3$), 1.55-1.80 (2H, m, $C\underline{H}_2$ AB<u>X</u>), 2.65-3.60 (16H, m, en and $C\underline{H}_2CO$), 3,99 and 4.30 (1H, dd, J = 17.4 and 17.1 Hz, C<u>H</u> AB<u>X</u>), 6.89 (1H, s, $C\underline{H}(Ph)_2$), 7.27-7.34 (10H, m, $CH(\underline{Ph})_2$). ^{13}C NMR (100.613 MHz, $CDCl_3$, TMS, δ(ppm)): 13.99 (1C, $CH_2CH_2CH_2CH_2\underline{C}H_3$), 22.48 (1C, $CH_2CH_2CH_2\underline{C}H_2CH_3$), 26.59 and 29.11 (2C, $\underline{C}H_2\underline{C}H_2CH_2CH_2CH_3$), 27.97 (6C, $C(\underline{C}H_3)_3$), 30.46 (1C, $\underline{C}H_2$ AB<u>X</u>), 31.63 (1C, $CH_2CH_2\underline{C}H_2CH_2CH_3$), 53.79-66.68 (8C, en and $\underline{C}H_2CO$), 62.91 (1C, <u>C</u>H AB<u>X</u>), 76.94 (1C, $\underline{C}H(Ph)_2$), 81.20 (2C, $\underline{C}(CH_3)_3$),

127.09-140.06 (12C, CH(Ph)$_2$), 170.76-172.66 (3C, CH_2CO and CHCO). m/z (ESI^+) calculated for $C_{39}H_{60}N_3O_6$ $(M+H)^+$ 666.448. Found 666.500.

2.2.15. 1,4,7-triazacyclononane-*N*-decanoate benzhydryl ester-*N'*-*N''*-diacetate *tert*-butyl ester (4d)

Compound **2d** (0.467 g, 1.12 mmol) was added to a solution of NO2AtBu (1,4,7-triazacyclononane-*N*,*N'*-diacetic acid *tert*-butyl ester) (0.401 g, 1.12 mmol) and K_2CO_3 (0.310 g, 2.25 mmol) in 30.0 mL of MeCN. The suspension was stirred during 4 h and was filtered to remove the solid. The yellow oil obtained after concentration under vacuum was purified by column chromatography (DCM/EtOH 7:3). Compound **4d** (0.753 g, 1.08 mmol) was obtained with a yield of 96.4%. ^{1}H NMR (300 MHz, $CDCl_3$, TMS, δ(ppm)): 0.88 (3H, t, J = 6.0 Hz, $(CH_2)_6CH_3$), 1.15-1.35 (12H, m, $(CH_2)_6CH_3$), 1.45 (18H, s, $C(CH_3)_3$), 1.52-1.83 (2H, m, CH_2 ABX), 2.60-4.00 (16H, m, en and CH_2CO), 4.32 (1H, t, CH ABX), 6.90 (1H, s, $CH(Ph)_2$), 7.27-7.36 (10H, m, $CH(Ph)_2$).

2.2.16. 1,4,7-triazacyclononane-*N*-hexadecanoate *tert*-butyl ester-*N'*-*N''*-diacetate *tert*-butyl ester (4e)

The title compound was prepared according to the method described for the preparation of **4a**, starting from **3e**. Compound **4e** (0.025 g, 0.037 mmol) was obtained with a yield of 12.3%. ^{1}H NMR (300 MHz, $CDCl_3$, TMS, δ(ppm)): 0.87 (3H, t, J = 6.9 Hz, $(CH_2)_{12}CH_3$), 1.24 (24H, s, $(CH_2)_{12}CH_3$), 1.45 (27H, s, $C(CH_3)_3$), 1.63-1.82 (2H, m, CH_2 ABX), 2.64-4.90 (17H, m, en, CH ABX and CH_2CO).

2.2.17. 1,4,7-triazacyclononane-*N*-hexadecanoate benzhydryl ester-*N'*-*N''*-diacetate *tert*-butyl ester (4f)

The title compound was prepared according to the method described for the preparation of **4d**, starting from **2f**. Compound **4f** (0.113 g, 0.145 mmol) was obtained with a yield of 74.0%. ^{1}H NMR (300 MHz, $CDCl_3$, TMS, δ(ppm)): 0.88 (3H, t, J = 6.3

Hz, $(CH_2)_{12}C\underline{H}_3$), 1.26 (24H, s, $(C\underline{H}_2)_{12}CH_3$), 1.45 (18H, s, $C(C\underline{H}_3)_3$), 1.50-1.83 (2H, m, $C\underline{H}_2$ AB$\underline{X}$), 2.60-4.40 (17H, m, en, $C\underline{H}$ AB$\underline{X}$ and $C\underline{H}_2CO$), 6.89 (1H, s, $C\underline{H}(Ph)_2$), 7.27-7.36 (10H, m, $CH(\underline{Ph})_2$).

2.2.18. 1,4,7-triazacyclononane-*N*-hexanoic-*N'*-*N''*-diacetic acid (NOTAC6)

5.00 mL of trifluoracetic acid (TFA) was added to a solution of **4a** (0.092 g, 0.174 mmol) in 5.00 mL of DCM and the reaction was stirred during 17 h. After that, the solvent and the remaining TFA were evaporated and the brown oil was washed three times with n-hexane to assure that all the TFA was removed. **NOTAC6** (0.090 mg, 0.128 mmol) was obtained with a yield of 73.6%. (The same method could be applied to the pro-chelators orthogonally protected). ^{1}H NMR (300 MHz, D_2O, DSS, pH = 1.31, δ(ppm)): 0.87 (3H, t, J = 7.0 Hz, $(CH_2)_2C\underline{H}_3$), 1.28-1.44 (4H, m, $(C\underline{H}_2)_2CH_3$), 1.75-1.98 (2H, m, $C\underline{H}_2$ AB$\underline{X}$), 3.28 (12H, s, en), 3.78 and 3.81 (1H, dd, J = 6.3 and 6.3 Hz, $C\underline{H}$ AB$\underline{X}$), 3.92 (4H, s, $C\underline{H}_2CO$). ^{13}C NMR (75.43 MHz, D_2O, DSS, pH = 1.31, δ(ppm)): 13.19 (1C, $(CH_2)_2\underline{C}H_3$), 22.08 (1C, $CH_2\underline{C}H_2CH_3$), 28.08 (1C, $\underline{C}H_2$ AB$\underline{X}$), 28.26 (1C, $\underline{C}H_2CH_2CH_3$), 47.13- 50.28 (6C, en), 55.99 (2C, $\underline{C}H_2CO$), 66.23 (1C, $\underline{C}H$ AB$\underline{X}$), 172.99 (2C, $CH_2\underline{C}O$), 175.38 (1C, $CH\underline{C}O$). m/z (ESI^+) calculated for $C_{16}H_{30}N_3O_6$ $(M+H)^+$ 360.21346. Found 360.21241.

2.2.19. 1,4,7-triazacyclononane-*N*-octanoic-*N'*-*N''*-diacetic acid (NOTAC8)

The title compound was prepared according to the method described for the preparation of **NOTAC6**, starting from **4c**. **NOTAC8** (0.034 g, 0.088 mmol) was obtained with a yield of 79.3%. ^{1}H NMR (300 MHz, D_2O, DSS, δ(ppm)): 0.82 (3H, t, J = 6.6 Hz, $(CH_2)_4C\underline{H}_3$), 1.24-1.44 (8H, m, $(C\underline{H}_2)_4CH_3$), 1.70-2.00 (2H, m, $C\underline{H}_2$ AB$\underline{X}$), 3.28 (12H, s, en), 3.79 (1H, t, J = 7.8 Hz, $C\underline{H}$ AB$\underline{X}$), 3.90 (4H, s, $C\underline{H}_2CO$). ^{13}C NMR (75.43 MHz, D_2O, DSS, δ(ppm)): 13.54 (1C, $(CH_2)_4\underline{C}H_3$), 22.11 (1C, $CH_2CH_2CH_2\underline{C}H_2CH_3$), 26.04 and 28.46 (2C, $\underline{C}H_2\underline{C}H_2CH_2CH_2CH_3$), 28.34 (1C, $\underline{C}H_2$

ABX), 30.96 (1C, $CH_2CH_2CH_2CH_2CH_3$), 47.35-50.40 (6C, en), 56.30 (2C, CH_2CO), 66.62 (1C, CH ABX), 173.04 (2C, CH_2CO), 175.32 (1C, CHCO). m/z (ESI^+) calculated for $C_{18}H_{33}N_3O_6$ $(M+H)^+$ 388.24. Found 388.50.

2.2.20. 1,4,7-triazacyclononane-*N*-decanoic-*N'*-*N''*-diacetic acid (NOTAC10)

The title compound was prepared according to the method described for the preparation of **NOTAC6**, starting from **4d**. **NOTAC10** (0.569 g, 0.751 mmol) was obtained with a yield of 88.4%. ^1H NMR (300 MHz, D_2O, DSS, δ(ppm)): 0.86 (3H, t_b, $(CH_2)_6CH_3$), 1.15-1.50 (8H, m_b, $(CH_2)_6CH_3$), 1.60-1.96 (2H, m_b, CH_2 ABX), 2.95-3.25 (12H, s_b, en), 3.57 (1H, s_b, CH ABX), 3.88 (4H, s_b, CH_2CO). ^{13}C NMR (75.43 MHz, D_2O, DSS, δ(ppm)): 13.87 (1C, $(CH_2)_6CH_3$), 22.62-31.98 (6C, $(CH_2)_6CH_3$), 28.60 (1C, CH_2 ABX), 46.64-50.93 (6C, en), 55.62 (2C, CH_2CO), 64.92 (1C, CH ABX), 171.95-172.28 (2C, CH_2CO), 174.93 (1C, CHCO). m/z (ESI^+) calculated for $C_{20}H_{38}N_3O_6$ $(M+H)^+$ 416.28. Found 416.50.

2.2.21. 1,4,7-triazacyclononane-*N*-hexadecanoic-*N'*-*N''*-diacetic acid (NOTAC16)

The title compound was prepared according to the method described for the preparation of **NOTAC6**, starting from **4e** or **4f**. **NOTAC16** (0.021 g, 0.029 mmol) was obtained with a yield of 78.4%. ^1H NMR (300 MHz, CD_3OD, TMS, δ(ppm)): 0.92 (3H, t, J = 6.6 Hz, $(CH_2)_{12}CH_3$), 1.31 (24H, s, $(CH_2)_{12}CH_3$), 1.70-2.20 (2H, m, CH_2 ABX), 2.80-3.37 (12H, m, en), 3.62 (1H, t, J = 7.2 Hz, CH ABX), 3.70-4.00 (4H, s_b, CH_2CO). m/z (ESI^+) calculated for $C_{26}H_{50}N_3O_6$ $(M+H)^+$ 500.36996. Found 500.36711.

2.2.22. [Al(NOTAC6)]

Aluminum nitrate and **NOTAC6** dissolved in water were added in equimolar amounts (Scheme 2). The pH was adjusted from 1.7 to 3.0 with 1 M KOH solution. The solution was stirred for 1 h at 75ºC. After it reached room temperature, the pH was fixed to 4.0. The water was evaporated and a 20.0 mM solution of the chelate in D_2O was

prepared to perform the multinuclear NMR characterization. ^{1}H NMR (300 MHz, D_2O, DSS, δ(ppm)): 0.92 (3H, t, J = 7.2 Hz, $(CH_2)_2C\underline{H}_3$), 1.32-1.50 (2H, m, $CH_2C\underline{H}_2CH_3$, 1.53-1.63 (2H, m, $C\underline{H}_2CH_2CH_3$), 1.75-1.90 and 2.04-2.16 (2H, m, $C\underline{H}_2$ AB<u>X</u>), 2.84-3.71 (13H, m, en and C<u>H</u> AB<u>X</u>), 3.82 (4H, d, J = 10.8 Hz, $C\underline{H}_2CO$). ^{13}C NMR (100.613 MHz, D_2O, $SiMe_4$, pH = 5.20, δ): 13.06 (1C, $(CH_2)_2\underline{C}H_3$), 22.04 (1C, $CH_2\underline{C}H_2CH_3$), 25.31 (1C, $\underline{C}H_2$ AB<u>X</u>), 29.09 (1C, $\underline{C}H_2CH_2CH_3$), 44.39- 54.06 (6C, en), 62.92 (2C, $\underline{C}H_2CO$), 68.61 (1C, <u>C</u>H AB<u>X</u>), 175.47 (2C, $CH_2\underline{C}O$), 176.94 (1C, CH<u>C</u>O). ^{27}Al NMR (104.261 MHz, H_2O/D_2O (75/25%), $[Al(H_2O)_6]^{3+}$, δ(ppm)): 47.58 ([Al(NOTAC6)]) ($\Delta\omega_{1/2}$ = 51.31 Hz).

2.2.23. [Ga(NOTAC6)]

Gallium nitrate and **NOTAC6** dissolved in water were added in equimolar amounts. The pH was adjusted from 1.8 to 5.7 with 1 M KOH solution. The solution was stirred for 1 h at 75ºC. The water was evaporated and a 20.0 mM solution of the chelate in D_2O was prepared to perform the multinuclear NMR characterization. ^{1}H NMR (300 MHz, D_2O, DSS, δ(ppm)): 0.93 (3H, t, J = 7.2 Hz, $(CH_2)_2C\underline{H}_3$), 1.26-1.51 (2H, m, $CH_2C\underline{H}_2CH_3$), 1.53-1.64 (2H, m, $C\underline{H}_2CH_2CH_3$), 1.70-1.90 and 2.06-2.18 (2H, m, $C\underline{H}_2$ AB<u>X</u>), 2.86-3.68 (13H, m, en and C<u>H</u> AB<u>X</u>), 3.83 (4H, d, J = 10.5 Hz, $C\underline{H}_2CO$). ^{13}C NMR (75.43 MHz, D_2O, DSS, pH = 5.20, δ): 13.21 (1C, $(CH_2)_2\underline{C}H_3$), 22.20 (1C, $CH_2\underline{C}H_2CH_3$), 25.91 (1C, $\underline{C}H_2$ AB<u>X</u>), 29.31 (1C, $\underline{C}H_2CH_2CH_3$), 44.05-53.84 (6C, en), 61.98 (2C, $\underline{C}H_2CO$), 68.67 (1C, <u>C</u>H AB<u>X</u>), 175.16 (2C, $CH_2\underline{C}O$), 176.85 (1C, CH<u>C</u>O). ^{71}Ga NMR (122.026 MHz, D_2O, $[Ga(H_2O)_6]^{3+}$, δ): 165.48 ([Ga(NOTAC6)]) ($\Delta\omega_{1/2}$ = 528.45 Hz). m/z (ESI^+) calculated for $C_{16}H_{26}GaN_3O_6K$ $(M+K)^+$ 464.07. Found 464.42.

2.2.24. [Al(NOTAC8)]

Aluminum nitrate and **NOTAC8** dissolved in water were added in equimolar amounts. The pH was adjusted from 1.9 to 2.7 with 1 M KOH solution. The solution was stirred for 1 h at 75ºC. After it reached room temperature, the pH was fixed to 4.1. The water was evaporated and a 4.28 mM solution of the chelate in D_2O was prepared to perform the multinuclear NMR characterization. ^{1}H NMR (300 MHz, D_2O, DSS, δ(ppm)): 0.88 (3H, t, J = 6.9 Hz, $(CH_2)_4C\underline{H}_3$), 1.22-1.67 (8H, m, $(C\underline{H}_2)_4CH_3$), 1.72-1.88 and 2.02-2.18 (2H, m, $C\underline{H}_2$ AB$\underline{X}$), 2.82-3.62 (12H, m, en), 3.67 (1H, t, J = 6.3 Hz, C$\underline{H}$ AB$\underline{X}$), 3.82 (4H, s, $C\underline{H}_2CO$). ^{13}C NMR (100.613 MHz, D_2O, DSS, δ(ppm)): 13.27 (1C, $(CH_2)_4\underline{C}H_3$), 21.79 and 30.72 (2C, $CH_2CH_2\underline{C}H_2\underline{C}H_2CH_3$), 25.50 (1C, $\underline{C}H_2$ AB$\underline{X}$), 26.80 and 28.24 (2C, $\underline{C}H_2\underline{C}H_2CH_2CH_2CH_3$), 44.56-54.18 (6C, en), 63.10 (2C, $\underline{C}H_2CO$), 68.82 (1C, $\underline{C}$H AB$\underline{X}$), 175.34 (2C, $CH_2\underline{C}O$), 176.63 (1C, CH$\underline{C}$O). ^{27}Al NMR (104.261 MHz, D_2O, $[Al(H_2O)_6]^{3+}$, δ(ppm)): 47.47 ([Al(NOTAC8)]) ($\Delta\omega_{1/2}$ = 54.87 Hz).

2.2.25. [Ga(NOTAC8)]

Gallium nitrate and **NOTAC8** dissolved in water were added in equimolar amounts. The pH was adjusted from 2.1 to 3.0 with 1 M KOH solution. The solution was stirred for 1 h at 75ºC. After it reached room temperature, the pH was fixed to 4.8. The water was evaporated and a 4.20 mM solution of the chelate in D_2O was prepared to perform the multinuclear NMR characterization. ^{1}H NMR (300 MHz, D_2O, DSS, δ(ppm)): 0.88 (3H, t, J = 6.9 Hz, $(CH_2)_4C\underline{H}_3$), 1.31-1.53 (8H, m, $(C\underline{H}_2)_4CH_3$), 1.75-1.90 and 2.05-2.20 (2H, m, $C\underline{H}_2$ AB$\underline{X}$), 2.90-3.55 (12H, m, en), 3.65 (1H, t, J = 5.7 Hz, C$\underline{H}$ AB$\underline{X}$), 3.83 (4H, m, $C\underline{H}_2CO$). ^{13}C NMR (100.613 MHz, D_2O, DSS, δ(ppm)): 13.27 (1C, $(CH_2)_4\underline{C}H_3$), 21.79 (1C, $CH_2CH_2CH_2\underline{C}H_2CH_3$), 26.03 (1C, $\underline{C}H_2$ AB$\underline{X}$), 26.85 and 28.23 (2C, $\underline{C}H_2\underline{C}H_2CH_2CH_2CH_3$), 30.71 (1C, $CH_2CH_2\underline{C}H_2CH_2CH_3$), 44.16-53.71 (6C, en), 61.95 (2C, $\underline{C}H_2CO$), 68.83 (1C, $\underline{C}$H AB$\underline{X}$), 174.79 (2C, $CH_2\underline{C}O$), 176.39 (1C,

CHCO). ^{71}Ga NMR (122.026 MHz, D_2O, $[Ga(H_2O)_6]^{3+}$, δ(ppm)): 165.75 ([Ga(NOTAC8)]) ($\Delta\omega_{1/2}$ = 621.80 Hz).

2.2.26. [Al(NOTAC10)]

Aluminum nitrate and **NOTAC10** dissolved in water were added in equimolar amounts. The pH was adjusted to 3.0 with 1 M KOH solution, occurring precipitation. The solution was stirred for 1 h at 75ºC. The water was evaporated and a solution of the solid in CD_3OD/D_2O (3:1) was prepared to perform the NMR characterization. ^{27}Al NMR (104.261 MHz, CD_3OD/D_2O (3:1), $[Al(H_2O)_6]^{3+}$, δ(ppm)): 47.31 ([Al(NOTAC10)]) ($\Delta\omega_{1/2}$ = 145.59 Hz).

2.2.27. [Al(NOTAC16)]

Method 1: Aluminum nitrate and **NOTAC16** dissolved in water were added in equimolar amounts. The pH was adjusted from 2.0 to 3.0 with 1 M KOH solution. The solution was stirred for 1 h at 75ºC. After it reached room temperature, the pH was fixed to 4.0. The water was evaporated and a solution of the solid in D_2O was prepared to perform the NMR characterization. ^{27}Al NMR (104.261 MHz, D_2O, $[Al(H_2O)_6]^{3+}$, δ(ppm)): no signal was found.

Method 2: Aluminum nitrate dissolved in water and **NOTAC16** dissolved in EtOH were added in equimolar amounts. The solution was stirred for 1 h at 75ºC. After it reached room temperature, the pH was fixed to 2.5 with 1 M KOH solution. The white precipitate formed with the addition of base was filtered off and the solution was evaporated. A solution of the solid in CD_3OD was prepared to perform the NMR characterization. ^{27}Al NMR (104.261 MHz, CD_3OD, $[Al(H_2O)_6]^{3+}$, δ(ppm)): 47.87 (weak signal).

2.2.28. [Ga(NOTAC16)]

Gallium nitrate dissolved in MeOH and **NOTAC16** dissolved in EtOH were added in equimolar amounts. The pH was adjusted from 0.8 to 2.8 with 1 M KOH solution. The solution was stirred for 1 h at 75ºC. The solvent was evaporated and a solution of the solid in CD_3OD was prepared to perform the NMR characterization. ^{71}Ga NMR (122.026 MHz, CD_3OD, $[Ga(H_2O)_6]^{3+}$, δ(ppm)): no signal was found.

2.3. Determination of the critical micellar concentration

The chelates were prepared by adding an appropriate amount of metal nitrate to a weighted quantity of ligand, dissolving in water at pH 4 and heating at 75°C during one hour. The water was evaporated and the solid was re-dissolved in phosphate buffer pH 7.4 or D_2O. In order to know the exact number of ligand equivalents existing in a weighted amount of ligand, an excess of a standard Al(III) solution was added to a weighted quantity of chelator, leaving the complexation to occur during one hour at 75°C. To this solution was added an excess of standard EDTA solution and this was back-titrated with a standard Ca(II) solution using eriochrome black T as indicator [28].

2.3.1. ^{27}Al NMR method

The determination of the critical micellar concentration (cmc) was performed by monitoring the variation of the half-width of the ^{27}Al NMR signal with the variation of the chelate concentration [4]. Stock solutions of [Al(NOTAC6)] and [Al(NOTAC8)] in D_2O, 13.0 mM and 4.28 mM respectively, were prepared at room temperature at pH 4.0. These concentrations were close to the limit of solubility of the chelates. The stock solutions were then gradually diluted in D_2O and ^{27}Al NMR spectra were recorded for each concentration of chelate.

2.3.2. Fluorescence method

The estimation of the critical micellar concentration (cmc) was also performed by fluorescence using 8-anilinonaphthalene-1-sulfonate (ANS) as fluorescence probe

[29]. Stock solutions of 16.63 mM of [Ga(NOTAC6)] and 3.36 mM of [Ga(NOTAC8)] were prepared in 0.1 M and 0.2 M phosphate buffer pH 7.4, respectively. These concentrations were close to the limit of solubility of the chelates. Solutions with different chelate concentrations, prepared by dilution of the stock solutions, containing $1x10^{-5}$ M ANS were used in this study. The fluorescence was measured at 480 nm upon excitation at 350 nm at room temperature. The fluorescence measurements were recorded on a Bio-Tek® Synergy™ HT spectrofluorimeter using the software KC4™.

2.4. Radiochemistry

[^{67}Ga] chelates for *in vivo* and *in vitro* experiments were prepared by adding 1 mCi of [^{67}Ga](citrate) to a solution of 1 mg of the chelator in HEPES (0.150 mL, 0.1 M, pH 5) and heated at 80ºC for ca 1 h. The radiochemical purity of the [^{67}Ga]L solutions were determined by thin layer chromatography (TLC), and the percentage of bound metal averaged 96%.

2.4.1. Determination of logP and stability in blood serum

The octanol/water partition coefficient (logP) of [^{67}Ga](NOTAC6) and [^{67}Ga](NOTAC8) was determined using the *shake-flask* method. The partition coefficient was determined by adding 25 μL of the chelate solution to a tube containing 1 mL of saline solution and 1 mL of 1-octanol. The resulting mixture was shaken at room temperature for 1 h and then centrifuged at 3000 rpm during 3 min. After the centrifugation, 100 μL of each phase was collected and the activity was measured. The partition coefficient was calculated as a ratio of the counts in the octanol fraction to the counts in the water fraction being this the result of the average of 5 determinations (S.D. < 0.01).

For the blood serum stability studies, 5 μCi of the standard solution of [^{67}Ga](NOTAC8) were added to 5 mL of fresh human serum, previously equilibrated in

5% CO_2 (95% air) environment at 37ºC. The mixture was stored in the same environment conditions, and aliquots of 100 mL (in triplicate) were taken at appropriate periods of time (0 min, 30 min, 1 h and 3 h). The aliquots were treated with 200 μL of ethanol, cooled (4ºC), and centrifuged during 15 min at 4000 rpm, at 4ºC, in order to precipitate the serum proteins. A 100 μL aliquot of supernatant was collected for activity counting in a γ well-counter. The sediment was washed twice with 1 mL of EtOH and its activity was counted. The activity of the supernatant was compared to that of the sediment in order to determine the percentage of the chelate associated to the proteins. The activity of the supernatant at 3 h was evaluated by TLC in order to check whether the chelate remained intact.

2.4.2. Biodistribution

Methods: A gamma camera-computer system (GE 400 GenieAcq, from General Electric, Milwaukee, WI, USA) was used for acquisition and pre-processing the *in vivo* gamma imaging. Data processing and display were performed on a personal computer using homemade software developed for the IDL 6.3 (Interactive Data Language, Research Systems, Boulder, CO, USA) computer tool.

Biodistribution studies: Groups of four animals (Wistar rat males weighting ca 200 g) were anaesthetized with Ketamine (50.0 mg/ml)/chloropromazine (2.5%) (10:3) and injected in the tail vein with ca 100 μCi of the tracer and sacrificed 30 min and 24 h later. The major organs were removed, weighted and counted in a γ well-counter.

In vivo gamma imaging: The animals were positioned in ventral decubitus over the detector. Image acquisition was initiated immediately before radiotracer injection in the tail vein. Sequences of 30 images (of 60 s each), were acquired to 64×64 matrices. In addition, static data were acquired 24 h after the radiotracer injection (180X180 matrices, time = 10 min). Images were subsequently processed using an IDL based

program. In order to analyze the transport of radiotracer over time, three regions of interest (ROI) were drawn on the image files, corresponding to the thorax, liver and left kidney. From these regions, time-activity curves were obtained and normalized to the maximum activity in all the organs.

3. Results and discussion

3.1. Synthesis

We followed two different synthetic approaches for the preparation of the chelators. In the first method both alkylating agents were protected in the form of *tert*-butyl ester, which allowed obtaining pro-chelators **4a** and **4e** (C and D in Scheme 1). Their reaction with TFA afforded the chelators NOTAC6 and NOTAC16. The other method involved the mono-alkylation of the triazacyclononane moiety using the alkylating agents protected in the form of benzhydryl ester (C in Scheme 1) originating intermediates **3b** and **3c**. Their reaction with 2-bromoacetate *tert*-butyl ester afforded the pro-chelators **4b** and **4c**, which are orthogonally protected. Treating **4b** and **4c** with TFA afforded the totally unprotected chelators NOTAC6 and NOTAC8. As the preparation of the mono-alkylated intermediates involves low yield synthesis we alternatively started with NO2AtB (a triazacyclononane moiety with two acetate pendant arms protected with *tert*-butyl groups) shortening the synthetic pathway and affording the pro-chelators **4d** and **4f** in good yield (E in Scheme 1). Their treatment with TFA afforded the chelators NOTAC10 and NOTAC16.

3.2. Characterization of the Al(III) and Ga(III) chelates by multinuclear NMR

Octahedral metal chelates of NOTA can have two possible arrangements for the coordination of the acetate groups, while the ethylenic bridges of the macrocyclic ring can also adopt two different orientations [30]. According to this, the chelates of NOTA

become chiral. Depending on the torsion angle of the acetate groups, the isomers can be clockwise (Δ) or anticlockwise (Λ). The orientation of the ethylenic bridges originates the isomers δ and λ. Therefore, two enantiomeric pairs are possible: type I [Δ(λλλ) and Λ(δδδ)] and type II [Δ(δδδ) and Λ(λλλ)]. The solid state structures of Ga(NOTA) and Al(NOTA) have been previously determined [6, 31], showing coordination of the metal ion to the three ring nitrogen atoms, as well as to three carboxylate oxygen atoms, yielding a pseudo-octahedral arrangement corresponding to the type I enantiomeric pair. The introduction of the aliphatic chain in the structures of the ligands produces a chiral carbon (*R* and *S* configurations), leading to another factor for enantiomerism. Accordingly, each of the chelates of NOTAC6, NOTAC8, NOTAC10 and NOTAC16 may originate four diastereoisomeric pairs of enantiomers in solution.

The ^{1}H NMR results obtained for the Al(III) and Ga(III) chelates of NOTAC6 and NOTAC8 in aqueous solution (illustrated in Figures 1, S3 – S4 for NOTAC8) are in agreement with the structures determined for the respective NOTA chelates by X-ray crystallography. These systems show symmetrical and well resolved resonances corresponding to the ring protons which create AA'MM' multiplet patterns arising from the (λλλ)↔(δδδ) ring conformational interconvertions. The β-CH_2 protons on the alkyl side chain become unequivalent upon coordination. The very similar patterns in the ^{1}H NMR spectra of the Al(III) and Ga(III) chelates of NOTAC6 and NOTAC8 observed at two different temperatures (25°C and 75°C, see Figures 1, S3 – S4) are consistent with a slow exchange regime and with the high rigidity of NOTA-based systems in solution, with two possible configurational arrangements for the coordinated acetate groups and the puckering of the ethylenediamine metal-chelate rings [30]. The ^{1}H NMR spectra recorded at chelate concentrations above and below the cmc show no differences

(Figure S4), indicating that the dynamic behavior of the chelates is not influenced by the micellization.

Despite the fact that it was not possible to obtain mono crystals suitable for X-ray diffraction, some useful structural information about the coordination site of the cations can be obtained from metal NMR data. The ^{27}Al and ^{71}Ga NMR chemical shifts of the chelates in aqueous solution (Table 1) are within the range usually found for octahedral or pseudo-octahedral species with a C_3 symmetry axis, responsible for the high symmetry at the coordination metal centre [4]. X-ray crystallography studies of Al(III) and Ga(III) chelates of NOTA [3, 31-34] and NOTA-based ligands [35-37] showed that these chelates have pseudo-octahedral geometries.

The complexation process of the metal ions with NOTAC10 and NOTAC16 was limited by the poor water solubility of the ligands, as monitored by the ^{27}Al NMR spectra. The [Al(NOTAC10)] complex was formed in aqueous solution, originating a ^{27}Al NMR signal at 47.31 ppm, much weaker than the main resonance from $[Al(H_2O)_6]^{3+}$ (0 ppm). NOTAC16 had very poor solubility in water and it was not possible to obtain the Al(III) and Ga(III) chelates in aqueous solution. However, when the Al(III) chelate was prepared in ethanol, a weak ^{27}Al NMR signal at 47.87 ppm could be detected.

The ^{27}Al NMR signals of the Al(III) chelates bearing short side chains (NOTAC6 and NOTAC8) show half-widths ($\Delta\omega_{1/2}$) similar to those found for the Al(III) chelate of NOTA, but they become significantly broader for the chelates with longer side chains [38]. Such an increased broadening with side chain length increase is more marked for the ^{71}Ga resonance of the Ga(III) complexes [36] (Table 1). These observations result from the quadrupolar relaxation of the metal nuclei and the slowing down of the rotational dynamics of the heavier complexes in solution.

3.3. Determination of the critical micellar concentration

The amphiphilic behavior of the metal chelates of NOTAC6 and NOTAC8 was demonstrated by determining their critical micellar concentration. For this purpose, two distinct methods were used. In one method, the fluorescence of ANS (8-anilino-1-naphtalene sulfonic acid), which is sensitive to the polarity of the environment, showing no fluorescence in water and high fluorescence in non-polar environments, was used as a probe for the Ga(III) chelates. Entrapping ANS in the inner part of the micelle, which is non-polar, increases the intensity of its fluorescence [29]. The cmc value was estimated by linear least-square fitting of the fluorescence emission at 480 nm versus the concentration of the chelates (Figure 2). The calculated cmc values were 5.20 mM for [Ga(NOTAC6)] and 0.36 mM for [Ga(NOTAC8)], showing that the two chelates have quite different aggregation behaviors, as an increase of alkyl chain length from four to six carbons decreases the cmc by an order of magnitude, reflecting a strong increase of the self-aggregation capacity of the chelates. The fact that the fluorescence intensity of the [Ga(NOTAC6)] system increases with the increase of concentration of chelate until the cmc value is reached suggests the formation of pre-micellar aggregates, contrary to what happens for [Ga(NOTAC8)]. The existence of pre-micellar aggregation has been detected before [23], by using DLS to prove the existence of aggregates of $[Gd(EPTPAC_{16})]^{2-}$ ($EPTPAC_{16}$ = (hydroxymethylhexadecanoyl ester) ethylenepropylenetriaminepentaacetic acid) with dimensions superior to 100 nm below the cmc. The formation of aggregates at concentrations below the cmc was also verified by fluorescence correlation spectroscopy in such reduced amount that the conventional techniques were not able to detect it [39].

On the other hand, the cmc values of [Al(NOTAC6)] and [Al(NOTAC8)] were assessed using ^{27}Al NMR spectroscopy. Due to the quadrupolar nature of the ^{27}Al

nuclide, whose nuclear relaxation is dependent on the rotational correlation time of the chelate in solution [4], the linear least-square fitting of the plot of the half-width of the ^{27}Al NMR signal as a function of the chelate concentration (Figure 3) allowed obtaining the cmc values. The plot for [Al(NOTAC8)], with a single break, reflected a simple micellization process with a cmc value of 0.25 mM, consistent with the value found by fluorescence for the analogous Ga(III) chelate. The corresponding plot for [Al(NOTAC6)] showed two breaks, at 1.16 mM and 4.30 mM, reflecting a more complex micellization behavior. While the second value (4.30 mM) corresponds quite well to the cmc value detected for the Ga(III) complex by fluorescence, the first value (1.16 mM) suggests the formation of pre-micellar aggregates in solution, in agreement with what has been found by fluorescence for the corresponding Ga(III) complex.

The cmc values obtained for the studied chelates are within the range of those found for amphiphilic Ni(II) chelates of triaza-based ligands with comparable alkyl chain lengths [40].

3.4. Determination of logP (and stability in blood serum)

The measured octanol/water partition coefficients (logP) of [^{67}Ga](NOTAC6) and [^{67}Ga](NOTAC8), respectively logP = -2.25 and logP = -1.19, revealed that the chelates present low lipophilicity which, as expected, increases when the chain length of the α-alkyl substituent at one of the pendant acetate arms increases from C4 to C6.

3.5. Stability in blood serum

Incubation studies of [^{67}Ga](NOTAC8) in fresh human serum, followed by precipitation of its protein content, showed that the percentage of the activity in the protein pellet steadily increased with the incubation time (13.8% at 30 min, 30.8% at 60 min), reaching a value of 36.7% at 3 h. This increasing activity associated to the blood proteins reflects the hydrophobic interactions involving the α-alkyl substituent at one of

the acetate pendant arms and hydrophobic regions of the proteins. Nevertheless, it was found by TLC analysis that the radioactivity present in this fraction, after 3 h of incubation, represents the intact radiochelate, reflecting the high stability of [^{67}Ga](NOTAC8) with regard to transchelation.

3.6. Biodistribution and imaging studies

The biodistribution data for [^{67}Ga](NOTAC8) and [^{67}Ga](NOTAC6) are expressed as the percentage of injected dose per gram of tissue (%ID/g) in Figure 4. Both chelates are excreted by kidneys but the hepatobiliary pathway (stated as the sum of liver and intestines) has also a strong contribution. This is particularly evident from the scintigraphic studies. However, from our results, [^{67}Ga](NOTAC8) seems to be more hepatospecific (1.28% of the activity is present in hepatobiliary transit at 30 min) than the corresponding C6 compound (hepatobiliary contribution at the same time equals 0.26%). These findings correlate with the higher lipophilicity of [^{67}Ga](NOTAC8). This chelate also shows a much higher lung uptake than [^{67}Ga](NOTAC6) chelate at 30 min, which is not persistent at longer times, as opposed to what has been found for the long chain tracer [^{153}Sm](EPTPAC$_{16}$)]$^{2-}$ [23].

Scintigraphic γ images of Wistar rats were obtained as a function of time after injection of the [^{67}Ga](NOTAC6) tracer. Figure 5 compares the images obtained 2 min, 4 min and 24 h after injection of the radiotracer, where various organs are enhanced. Time–activity curves for the [^{67}Ga](NOTAC6) tracer (Figure 6) were obtained from scintigraphic dynamic acquisition experiments. The curves were smoothed and normalized in relation to the maximum radioactivity obtained. From these curves one can notice that the activity increased sharply in the thorax, liver and kidneys immediately after the injection, possibly corresponding essentially to blood activity. The highest value for liver and thorax was obtained after one minute, while it took

about two minutes to reach maximum activity at the kidneys. After reaching this maximum, the radioactivity in the liver and thorax decayed relatively slowly while for the kidneys it was almost constant during all the acquisition. At 30 min, the activity at the kidneys remained at 99% of the maximum attained while for liver and kidneys these values were 69% and 38%, respectively. We obtained the same information from the images presented in Figure 5 where only the kidneys and bladder are clearly visible. From these findings we can conclude that at least for [^{67}Ga](NOTAC6), despite the contribution of the hepatobiliary mechanism for the radiotracer elimination, the main excretion mechanism is the kidney pathway. This is in accordance with the logP obtained for [^{67}Ga](NOTAC6).

From the biodistribution data (for the two compounds) and from the imaging results for the NOTAC6 radiotracer, it is noticeable that most of the radioactivity was cleared off from tissues and organs within 24 h with virtually no deposition in the bones and liver/spleen, demonstrating the high *in vivo* stability of [^{67}Ga](NOTAC6) and [^{67}Ga](NOTAC8).

From the specifications of the supplier of [^{67}Ga](citrate) (CIS-BIO, Gift-sur-Yvette, France), less than 4.5 ng of Ga(III) (1 mCi) of Ga(III) should be present in the final solution of [^{67}Ga](NOTAC8) or [^{67}Ga](NOTAC6). Thus, in both cases, the concentrations were well below the cmc determined for the complexes, and no micelles were supposed to be present in solution.

4. Conclusions

We developed a small library of four amphiphilic NOTA-based chelators presenting a α-alkyl chain of variable size. The synthetic strategy that was used in this work may also be compatible with the preparation of bifunctional chelators which can be covalently coupled to targeting biomolecules bearing an amine function (eg. peptides). This is of paramount importance regarding receptor mediated medical imaging and radiotherapeutic applications.

The metal chelates of NOTAC6 and NOTAC8 show distinct amphiphilic behavior. The shorter-size-chain chelate shows some level of pre-aggregation additionally to the formation of micelles. When the α-alkyl chain has more than six carbon atoms, the chelators show low solubility in water, thus reducing the possibility of using their neutral chelates in biological applications.

The increase in the size of the α-alkyl chain, and the corresponding increase in the lipophilicity of the chelates (logP values), are responsible for a higher uptake of the Ga(III) chelates in the liver. From the imaging and biodistribution studies we can conclude that [^{67}Ga](NOTAC8) and [^{67}Ga](NOTAC6) present high *in vivo* stability and are excreted quite quickly, co-existing the kidney and hepatobiliary pathway.

The fact that the radiolabeled chelates were injected at concentrations below the determined cmc, precluded the formation of micelles *in vivo* with consequent lower hepatic uptake than expected.

5. Abbreviations

%ID/g = percentage of injected dose per gram of tissue

ANS = 8-anilino-1-naphtalene sulfonic acid

cmc = critical micellar concentration

DLS = dynamic light scattering

EDTA = ethylenediaminetetraacetic acid

$EPTPAC_{16}$ = (hydroxymethylhexadecanoyl ester) ethylenepropylenetriaminepentaacetic acid

HEPES = *N*-(2-Hydroxyethyl)piperazine-*N'*-(2-ethanesulfonic acid)

IDL = interactive data language

L = ligand

MRI = Magnetic Resonance Imaging

NO2AtB = 1,4,7-triazacyclononane-*N*,*N'*-diacetic acid *tert*-butyl ester

NODASA = 1,4,7-triazacyclononane-*N*-succinic acid-*N'*,*N''*-diacetic acid

NOTA = 1,4,7-triazacyclononane-*N*,*N'*,*N''*-triacetic acid

NOTAC6 = 1,4,7-triazacyclononane-*N*-hexanoic acid-*N'*,*N''*-diacetic acid

NOTAC8 = 1,4,7-triazacyclononane-*N*-octanoic acid-*N'*,*N''*-diacetic acid

NOTAC10 = 1,4,7-triazacyclononane-*N*-decanoic acid-*N'*,*N''*-diacetic acid

NOTAC16 = 1,4,7-triazacyclononane-*N*-hexadecanoic acid-*N'*,*N''*-diacetic acid

PET = positron emission tomography

ROI = regions of interest

Tf = transferrin

TFA = trifluoracetic acid

TLC = thin layer chromatography

Acknowledgements

We thank the support from Fundação para a Ciência e a Tecnologia (F.C.T.), Portugal, (project PTDC/QUI/70063/2006) and FEDER. The Bruker Avance III 400 NMR spectrometer in Braga was acquired with the support of the Programa Nacional de Reequipamento Científico of the F.C.T., Portugal (contract REDE/1517/RMN/2005 - as

part of RNRMN - Rede Nacional de RMN). This work was carried out in the framework of the COST D38 Action and EU-FP6 “Network of Excellence” EMIL (grant no. LSHC-2004-503569) project.

Supplementary information: Structure and labeling of protons used to assign the ^{1}H NMR resonances of the non-labile protons of NOTAC8 (Figure S1); ^{1}H NMR spectra of NOTAC8 (25ºC, pH 1.41) (Figure S2), [Ga(NOTAC8)] (25ºC, pH 4.00) (Figure S3) and [Al(NOTAC8)] (25ºC, pH 4.00, at 4.28 mM and 0.15 mM) (Figure S4).

References

[1] M. Fani, J.P. André, H.R. Maecke, Contrast Media and Molecular Imaging 3 (2008) 67-77.

[2] W.R. Harris, V.L. Pecoraro, Biochemistry 22 (1983) 292-299.

[3] C.J. Broan, J.P.L. Cox, A.S. Craig, R. Kataky, D. Parker, A. Harrison, A.M. Randall, G. Ferguson, Journal of the Chemical Society-Perkin Transactions 2 (1991) 87-99.

[4] J.P. André, H.R. Mäcke, Journal of Inorganic Biochemistry 97 (2003) 315-323.

[5] R. Ma, M.J. Welch, J. Reibenspies, A.E. Martell, Inorganica Chimica Acta 236 (1995) 75-82.

[6] A.S. Craig, D. Parker, H. Adams, N.A. Bailey, Journal of the Chemical Society, Chemical Communications (1989) 1793-1794.

[7] M.I.M. Prata, A.C. Santos, C.F.G.C. Geraldes, J.J.P. de Lima, Nuclear Medicine and Biology 26 (1999) 707-710.

[8] M.I.M. Prata, A.C. Santos, C.F.G.C. Geraldes, J.J.P. de Lima, Journal of Inorganic Biochemistry 79 (2000) 359-363.

[9] J.P. André, H.R. Maecke, M. Zehnder, L. Macko, K.G. Akyel, Chemical Communications (1998) 1301-1302.

[10] J.P. André, H. Mäcke, A. Kaspar, B. Kunnecke, M. Zehnder, L. Macko, Journal of Inorganic Biochemistry 88 (2002) 1-6.

[11] J. Notni, K. Pohle, J.A. Peters, H. Gorls, C. Platas-Iglesias, Inorg Chem 48 (2009) 3257-3267.

[12] E.T. Clarke, A.E. Martell, Inorganica Chimica Acta 181 (1991) 273-280.

[13] H.R. Maecke, J.P. André, in: PET Chemistry The Driving Force in Molecular Imaging, Springer, 2006.

[14] S.M. Moghimi, A.C. Hunter, J.C. Murray, Pharmacological Reviews 53 (2001) 283-318.

[15] V.P. Torchilin, A.N. Lukyanov, Z. Gao, B. Papahadjopoulos-Sternberg, Proceedings of the National Academy of Sciences of the United States of America 100 (2003) 6039-6044.

[16] J. Wang, D. Mongayt, V.P. Torchilin, Journal of Drug Targeting 13 (2005) 73-80.

[17] V.P. Torchilin, Adv Drug Deliv Rev 54 (2002) 235-252.

[18] K. Kostarelos, D. Emfietzoglou, Journal of Liposome Research 9 (1999) 429-460.

[19] W.J. Mulder, G.J. Strijkers, G.A. van Tilborg, A.W. Griffioen, K. Nicolay, NMR in Biomedicine 19 (2006) 142-164.

[20] G.M. Nicolle, E. Toth, K.P. Eisenwiener, H.R. Macke, A.E. Merbach, Journal of Biological Inorganic Chemistry 7 (2002) 757-769.

[21] S.M. Moghimi, A.E. Hawley, N.M. Christy, T. Gray, L. Illum, S.S. Davis, FEBS Lett 344 (1994) 25-30.

[22] V.S. Trubetskoy, M.D. Frank-Kamenetsky, K.R. Whiteman, G.L. Wolf, V.P. Torchilin, Acad Radiol 3 (1996) 232-238.

[23] S. Torres, M.I. Prata, A.C. Santos, J.P. André, J.A. Martins, L. Helm, E. Tóth, M.L. Garcia-Martin, T.B. Rodrigues, P. Lopez-Larrubia, S. Cerdan, C.F.G.C. Geraldes, NMR Biomed 21 (2008) 322-336.

[24] Z.R. Zhang, K.X. Liang, S. Bloch, M. Berezin, S. Achilefu, Bioconjugate Chem. 16 (2005) 1232-1239.

[25] K.S. Birdi, H.N. Singh, S.U. Dalsager, Journal of Physical Chemistry 83 (1979) 2733-2737.

[26] A. Riesen, T.A. Kaden, W. Ritter, H.R. Macke, Journal of the Chemical Society-Chemical Communications (1989) 460-462.

[27] J.B. Miller, Journal of Organic Chemistry 24 (1959) 560-561.

[28] J. Bassett, R.C. Denney, G.H. Jeffery, J. Mendham, in: Vogel's: Textbook of Quantitative Inorganic Analysis, Longman, New York, 1978.

[29] E. De Vendittis, G. Palumbo, G. Parlato, V. Bocchini, Anal Biochem 115 (1981) 278-286.

[30] M.J.V. Merwe, J.C.A. Boeyens, R.D. Hancock, Inorganic Chemistry 24 (1985) 1208-1213.

[31] U. Bossek, D. Hanke, K. Wieghardt, B. Nuber, Polyhedron 12 (1993) 1-5.

[32] A. Jyo, T. Kohno, Y. Terazono, S. Kawano, Analytical Sciences 6 (1990) 629-630.

[33] T.W. Duma, F. Marsicano, R.D. Hancock, Journal of Coordination Chemistry 23 (1991) 221-232.

[34] K. Wieghardt, U. Bossek, P. Chaudhuri, W. Herrmann, B.C. Menke, J. Weiss, Inorganic Chemistry 21 (1982) 4308-4314.

[35] J.P. André, Synthesis, Characterization and Applications Relevant to Magnetic Resonance Imaging and Radiopharmacy of New Complexes of Al(III), Ga(III) and Gd(III), Basel, 1999.

[36] E. Cole, R.C.B. Copley, J.A.K. Howard, D. Parker, G. Ferguson, J.F. Gallagher, B. Kaitner, A. Harrison, L. Royle, Journal of the Chemical Society-Dalton Transactions (1994) 1619-1629.

[37] D.A. Moore, P.E. Fanwick, M.J. Welch, Inorganic Chemistry 29 (1990) 672-676.

[38] M.P.M.M. Catarro, Estudos de Ligandos Poliazamacrocíclicos e de seus Complexos Metálicos, Coimbra, 1995.

[39] H. Zettl, Y. Portnoy, M. Gottlieb, G. Krausch, Journal of Physical Chemistry B 109 (2005) 13397-13401.

[40] P.C. Griffiths, I.A. Fallis, T. Chuenpratoom, R. Watanesk, Advances in Colloid and Interface Science 122 (2006) 107-117.

Table 1 – ^{27}Al and ^{71}Ga NMR chemical shifts and signal half-widths of Al(III) and Ga(III) chelates of NOTA derivatives in aqueous solution (25ºC) compared to those for NOTA.

	^{27}Al NMR		**^{71}Ga NMR**	
Ligand	δ (ppm)	$\Delta\omega_{1/2}$ (Hz)	δ (ppm)	$\Delta\omega_{1/2}$ (Hz)
NOTA	49 [38]	60 [38]	171 [36]	210 [36]
NOTAC6	47.6[a]	51.3	165.5[b]	528.5
NOTAC8	47.5[c]	55.0	165.8[d]	621.8
NOTAC10	47.3[e]	145.6	-	-
NOTAC16	47.9[f]	-	-	-

[a] 20.0 mM, pH 4.0; [b] 20.0 mM, pH 5.7; [c] 4.28 mM, pH 4.1; [d] 4.20 mM, pH 4.8; [e] Concentration not defined, pH 3.0; [f] Methanol solution with concentration not defined, pH 2.5.

Scheme 1 – A – i) Solution of TBTA in cyclohexane added to the bromoacid dissolved in DCM; ii) DMA; iii) $BF_3.OEt_2$. B – Solution of DDM in acetone added to the bromoacid dissolved in acetone. C – Addition of ester solution in DCM to the 1,4,7-triazacyclononane solution in DCM; D – K_2CO_3 and *tert*-butyl bromoacetate in MeCN; E – K_2CO_3 and NO2AtBu ester in MeCN; F – TFA/DCM (1:1).

Scheme 2 – A – $Al(NO_3)_3.9H_2O$ in H_2O; B – $Ga(NO_3)3.xH_2O$ in H_2O.

Figure 1 – A – ^{1}H NMR spectrum of [Al(NOTAC8)] (400 MHz, D_2O, 75ºC, pH 4.10). B – ^{1}H COSY spectrum of [Al(NOTAC8)].

Figure 2 – Fluorescence intensity of the ANS fluorophore at 480 nm versus: A – [Ga(NOTAC6)] concentration; B – [Ga(NOTAC8)] concentration. The cmc values are established from graphical break points.

Figure 3 – Half-width of the ^{27}Al NMR signal of Al(III) chelates versus chelate concentration: A – [Al(NOTAC6)]; B – [Al(NOTAC8)].

Figure 4 – Biodistribution profile for Wistar rats (percentage of the injected dose/g of organ) of [^{67}Ga](NOTAC6) (white bars) and [^{67}Ga](NOTAC8) (gray bars) at 30 min (A) and 24 h (B) after injection.

Figure 5 – Scintigraphic images at 2 min, 4 min and 24 h of a Wistar rat injected with [^{67}Ga](NOTAC6).

Figure 6 – Time/activity curves of [^{67}Ga](NOTAC6) obtained from dynamic images of the regions of interest of a Wistar rat. Kidneys (●); Liver (■); Thorax (▲).

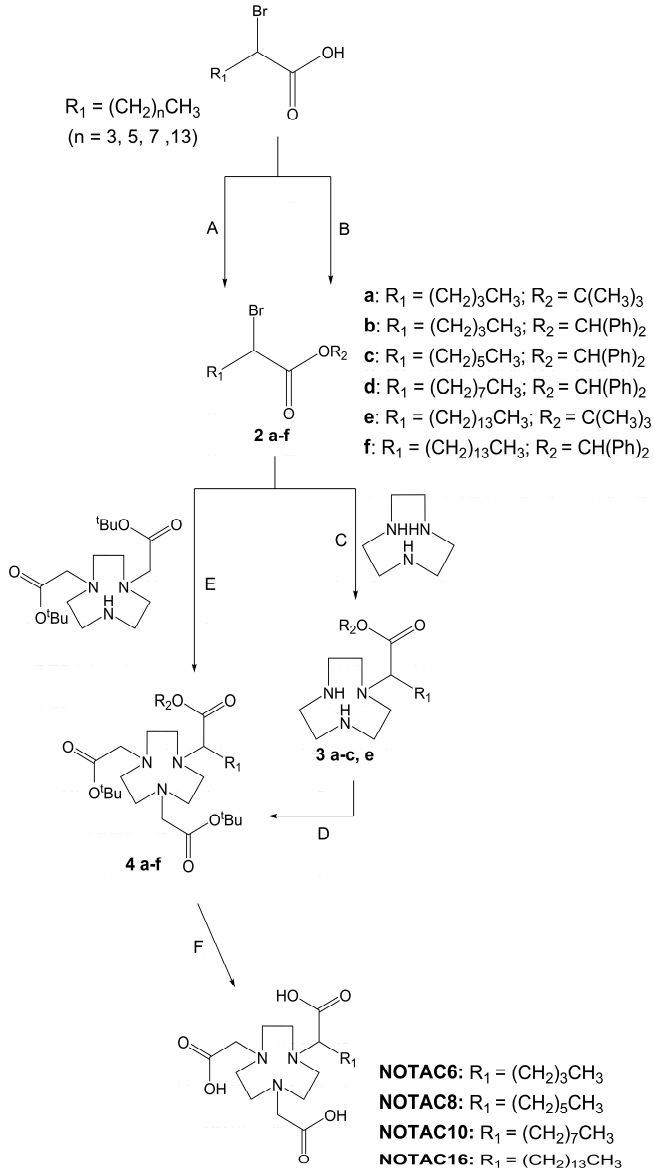
Br
OH
R1
O
R1 = (CH2)nCH3
(n = 3, 5, 7 ,13)
A
B
a: R1 = (CH2)3CH3; R2 = C(CH3)3
b: R1 = (CH2)3CH3; R2 = CH(Ph)2
c: R1 = (CH2)5CH3; R2 = CH(Ph)2
d: R1 = (CH2)7CH3; R2 = CH(Ph)2
e: R1 = (CH2)13CH3; R2 = C(CH3)3
f: R1 = (CH2)13CH3; R2 = CH(Ph)2
Br
OR2
R1
O
2 a-f
C
E
tBuO
O
O
OtBu
NHHN
H
N
R2O
O
NH
N
R1
H
N
3 a-c, e
R2O
O
R1
O
OtBu
N
N
N
OtBu
O
4 a-f
D
F
HO
O
O
OH
N
N
R1
N
OH
O
NOTAC6: R1 = (CH2)3CH3
NOTAC8: R1 = (CH2)5CH3
NOTAC10: R1 = (CH2)7CH3
NOTAC16: R1 = (CH2)13CH3

Scheme 1

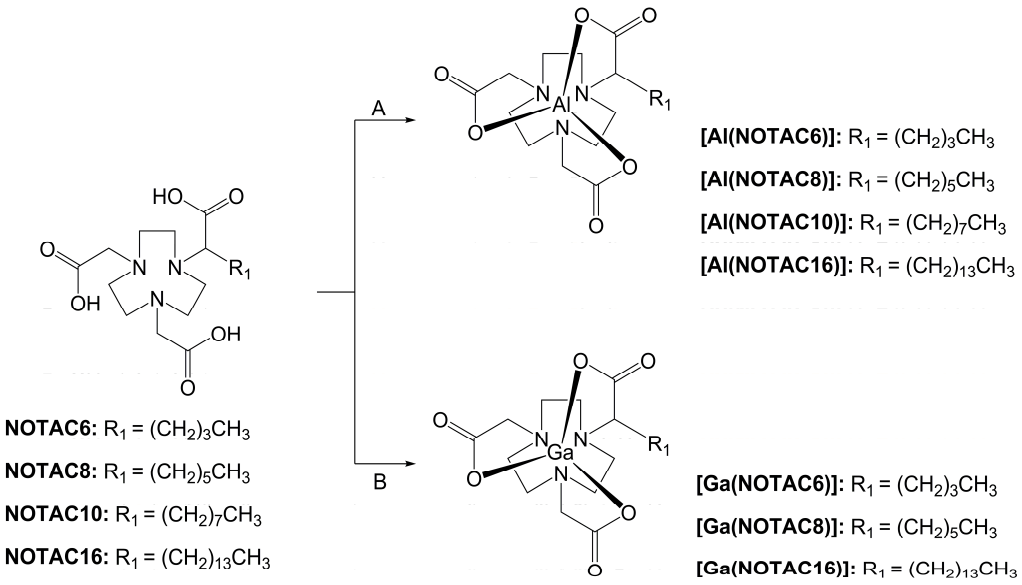
A
B
Al
Ga
[Al(NOTAC6)]: R1 = (CH2)3CH3
[Al(NOTAC8)]: R1 = (CH2)5CH3
[Al(NOTAC10)]: R1 = (CH2)7CH3
[Al(NOTAC16)]: R1 = (CH2)13CH3
[Ga(NOTAC6)]: R1 = (CH2)3CH3
[Ga(NOTAC8)]: R1 = (CH2)5CH3
[Ga(NOTAC16)]: R1 = (CH2)13CH3
NOTAC6: R1 = (CH2)3CH3
NOTAC8: R1 = (CH2)5CH3
NOTAC10: R1 = (CH2)7CH3
NOTAC16: R1 = (CH2)13CH3

Scheme 2

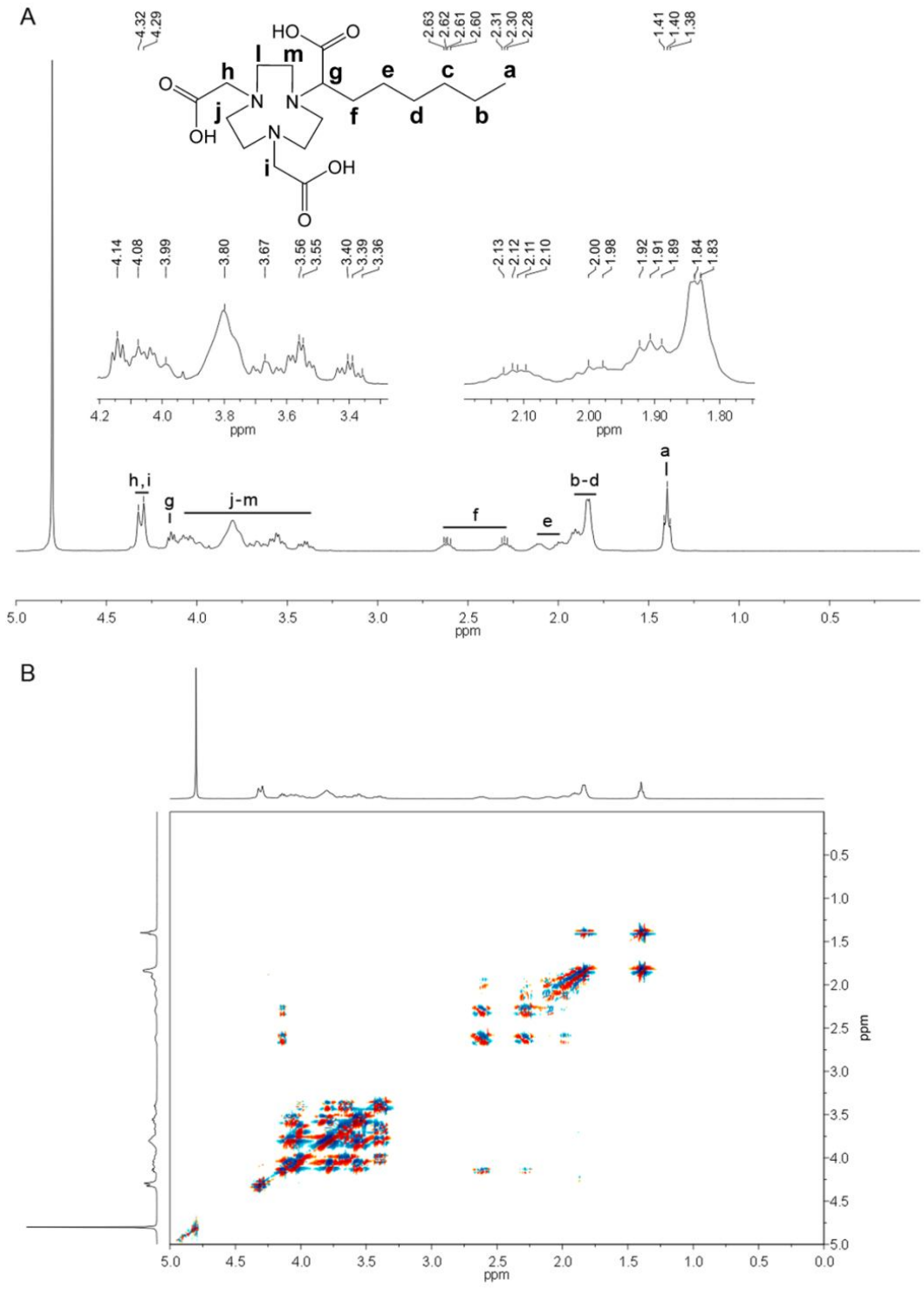
A
4.32
4.29
2.63
2.62
2.61
2.60
2.31
2.30
2.28
1.41
1.40
1.38
HO
O
l m
h
g
e
c
a
O
N
N
j
f
d
b
OH
N
i
OH
O
4.14
4.08
3.99
3.80
3.67
3.56
3.55
3.40
3.39
3.36
2.13
2.12
2.11
2.10
2.00
1.98
1.92
1.91
1.89
1.84
1.83
4.2
4.0
3.8
3.6
3.4
ppm
2.10
2.00
1.90
1.80
ppm
h,i
g
l
j-m
f
e
b-d
a
l
5.0
4.5
4.0
3.5
3.0
2.5
ppm
2.0
1.5
1.0
0.5
B
0.5
1.0
1.5
2.0
2.5
3.0
3.5
4.0
4.5
5.0
ppm
5.0
4.5
4.0
3.5
3.0
2.5
ppm
2.0
1.5
1.0
0.5
0.0

Figure 1

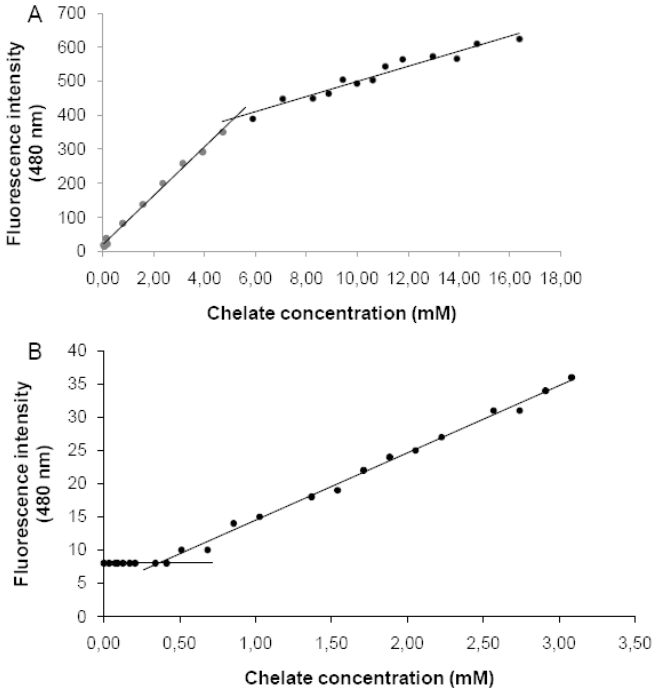
A
Fluorescence intensity (480 nm)
700
600
500
400
300
200
100
0
0,00 2,00 4,00 6,00 8,00 10,00 12,00 14,00 16,00 18,00
Chelate concentration (mM)
B
Fluorescence intensity (480 nm)
40
35
30
25
20
15
10
5
0
0,00 0,50 1,00 1,50 2,00 2,50 3,00 3,50
Chelate concentration (mM)

Figure 2

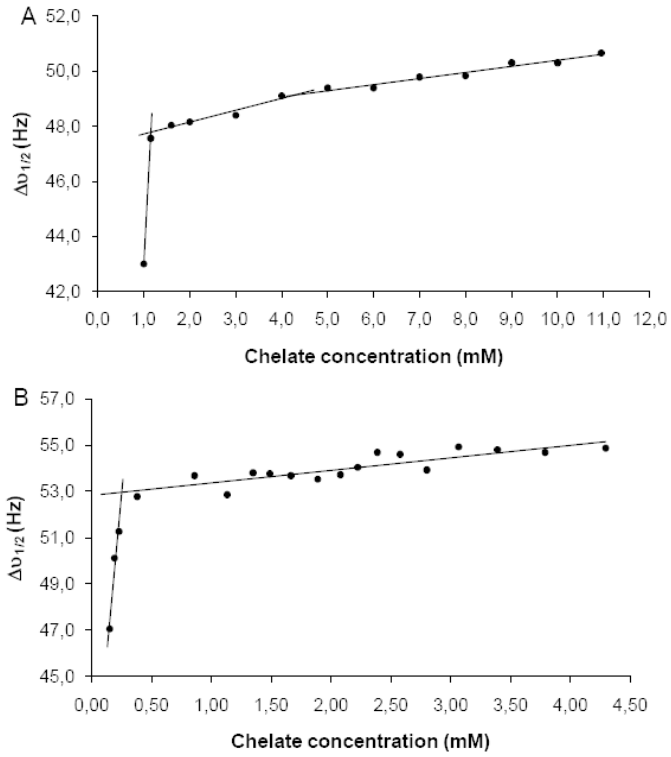
A
52,0
50,0
48,0
46,0
44,0
42,0
Δυ1/2 (Hz)
0,0 1,0 2,0 3,0 4,0 5,0 6,0 7,0 8,0 9,0 10,0 11,0 12,0
Chelate concentration (mM)
B
57,0
55,0
53,0
51,0
49,0
47,0
45,0
Δυ1/2 (Hz)
0,00 0,50 1,00 1,50 2,00 2,50 3,00 3,50 4,00 4,50
Chelate concentration (mM)

Figure 3

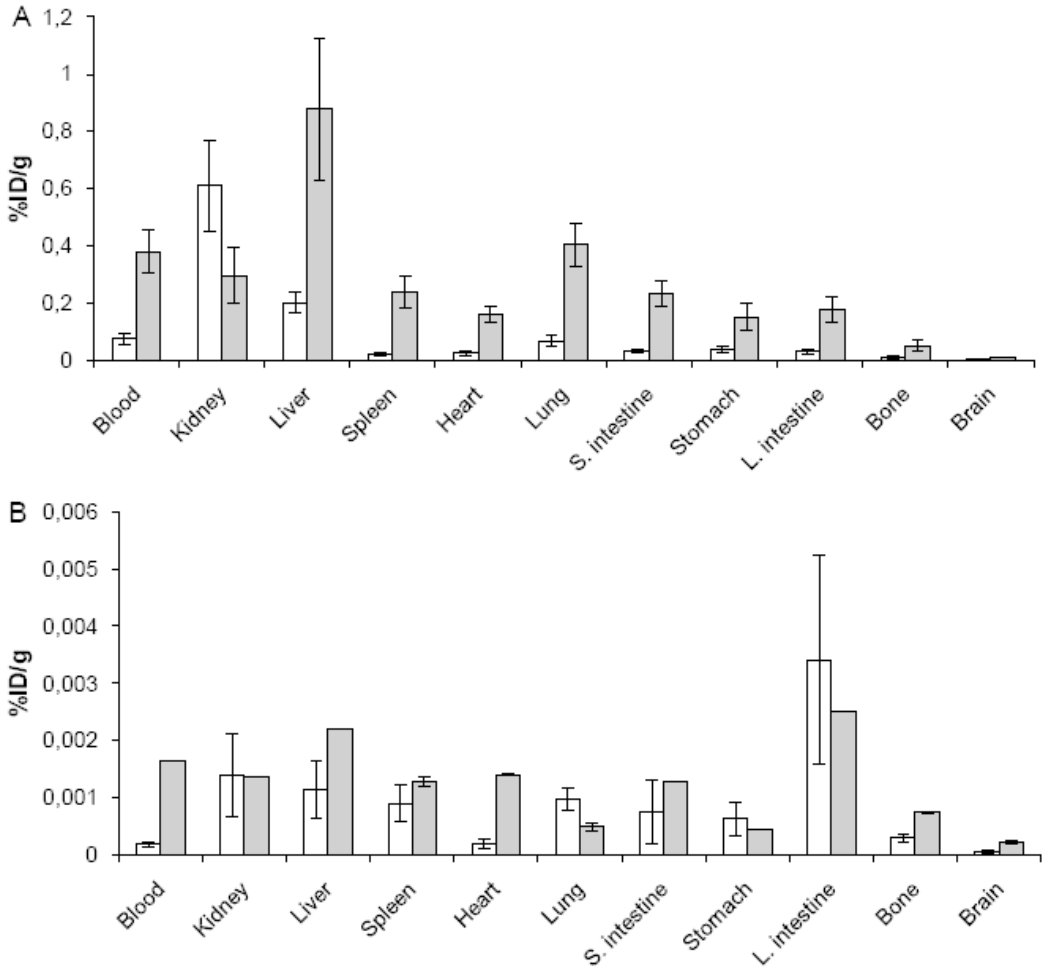
A
1,2
1
0,8
0,6
0,4
0,2
0
%ID/g
Blood
Kidney
Liver
Spleen
Heart
Lung
S. intestine
Stomach
L. intestine
Bone
Brain
B
0,006
0,005
0,004
0,003
0,002
0,001
0
%ID/g
Blood
Kidney
Liver
Spleen
Heart
Lung
S. intestine
Stomach
L. intestine
Bone
Brain

Figure 4

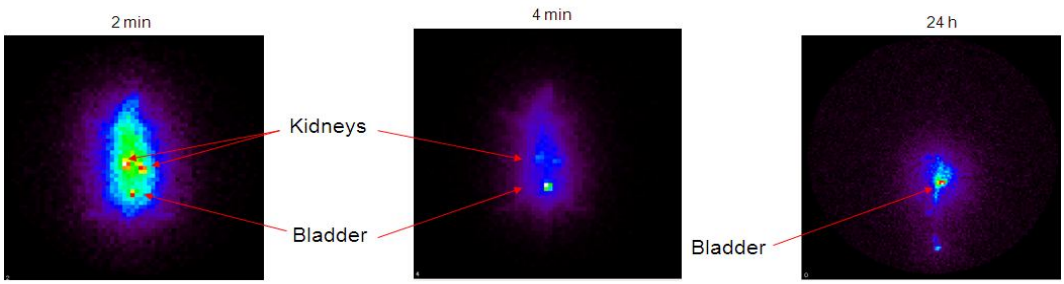

Figure 5

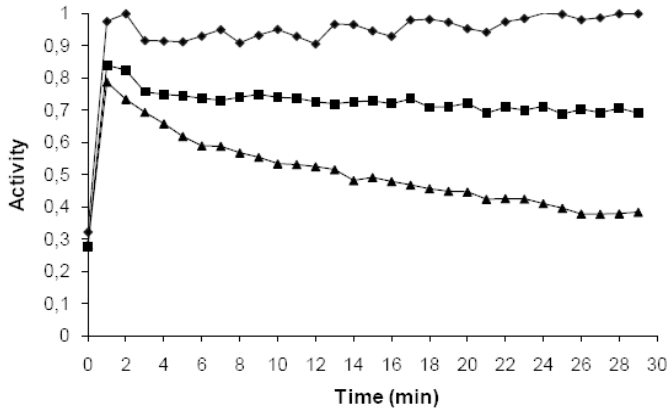
Activity
1
0,9
0,8
0,7
0,6
0,5
0,4
0,3
0,2
0,1
0
0 2 4 6 8 10 12 14 16 18 20 22 24 26 28 30
Time (min)

Figure 6